NASA-CR-204619

PROCEEDINGS REPRINT

SPIE—The International Society for Optical Engineering

Reprinted from

Space Processing of Materials

4–5 August 1996
Denver, Colorado

Volume 2809

conditions of low gravity where there would be less stirring taking place and the effective compositional gradient in

Directional Solidification of Mercury Cadmium Telluride During the Second United States Microgravity Payload Mission (USMP-2)

D. C. Gillies, S. L. Lehoczky, F. R. Szofran, D. A. Watring, H. A. Alexander* and G. A. Jerman

NASA Marshall Space Flight Center, Huntsville, AL 35812
* - USRA Research Associate

ABSTRACT

As a solid solution semiconductor having a large separation between liquidus and solidus, mercury cadmium telluride (MCT) presents a formidable challenge to crystal growers desiring an alloy of high compositional uniformity. To avoid constitutional supercooling during Bridgman crystal growth it is necessary to solidify slowly in a high temperature gradient region. The necessary translation rate of less than 1 mm/hr results in a situation where fluid flow induced by gravity on earth is a significant factor in material transport. The Advanced Automated Directional Solidification Furnace (AADSF) is equipped to provide the stable thermal environment with a high gradient, and the required slow translation rate needed. Ground based experiments in AADSF show clearly the dominance of flow driven transport. The first flight of AADSF in low gravity on USMP-2 provided an opportunity to test theories of fluid flow in MCT and showed several solidification regimes which are very different from those observed on earth. Residual acceleration vectors in the orbiter during the mission were measured by the Orbital Acceleration Research Experiment (OARE), and correlated well with observed compositional differences in the samples.

KEYWORDS: Microgravity, Crystal Growth, HgCdTe, Solidification, Fluid Flow, Furnace

2. INTRODUCTION

diffusion coefficient, or mass transport coefficient, it is possible to simulate diffusion controlled conditions and model the one dimensional compositional profile along an ingot of known length. The model illustrates initial and final transients. By this means it is possible to obtain reasonable values for the mass transport coefficient. It was found that a value of 5.5×10^{-5} cm^2/s is a good fit for a wide range of translation rates. Two typical compositional profiles are shown in figure 3. These were taken in a heat pipe furnace with a higher temperature gradient than in the AADSF and this was taken into account in the modeling, but the results clearly show that mass transport in this system is not dominated by convection. A complete mixing model would give very different results.

Frequently it is useful to interrupt a growth by rapidly removing the sample from the hot zone. This effectively quenches in the interface, and with the feedback of furnace position it is possible to locate the exact position and thermal environment of the growth process. Such quenches are normally done in the steady state region of the growth. As indicated in section 2 the interface is normally quite curved into the liquid at the center. A typical example is shown in figure 4. The information obtained demonstrates clearly one of the important features of solid solution semiconductors, namely that the interface is not an isotherm. The analysis of the material adjacent to this interface has been plotted in terms of solidification temperature rather than composition in figure 5. It can be seen that there is a differential of almost 20 degrees C across this interface.

4. THE USMP-2 EXPERIMENT

Prior to the USMP-2 experiment, 15 growth runs were made in the prototype furnace, two in the Ground Control Experimental Laboratory (GCEL), and two in the flight furnace. All furnaces were thermally profiled, and found to be close in characteristics; no set point changes were made to accommodate differences between them. AADSF is a five zone furnace with primary hot and cold zones separated by a thermal barrier which acts as an

instrument location are transposed to the AADSF position. As can be seen, the first attitude was of very low total residual acceleration, but the vector in the Z direction points from the solid to the liquid. The second attitude has a large component caused by the gravity gradient effect of the AADSF being 13 feet above the c.g., but the vector normal to the interface is stabilizing from liquid to solid. The final attitude also has the large transverse vector, and in this case has the destabilizing component from solid to liquid.

Figure 7 illustrates the history of the growth of the mercury cadmium telluride in terms of the mission timeline. The top scale is in Mission Elapsed Time (MET), and tells in days, hours and minutes the duration of the mission from launch. The y-axis shows the cadmium telluride mole fraction (x in $Hg_{1-x}Cd_xTe$), while the x-axis is from measured values along the crystal. The solid line is a modeled diffusion controlled composition profile based on the D value shown. Post growth analysis indicated a supercooled region of 2.2 cm and this has been taken into account during the modeling. This distance is longer than the ground based crystals demonstrate. The MET scale is not linear, because the growth rate is not linear; it has been plotted to simulate the real time for a given distance, and in particular those times at which attitude changes took place. The translation rate used was 0.79 mm/hr, which was thought to be slow enough to avoid constitutional supercooling even in the space environment with no stirring adjacent to the interface. To provide a time indication of the changes in attitude, it was decided to increase the translation rate by a factor of 15 for 5 minutes, followed by a return to the initial rate. This change was made at MET 6/15:37 and was planned to give 4 hours of "recovery" time prior to the attitude change shown in figure 8. This would involve a translation of almost 1mm in five minutes. It was anticipated that breakdown and dendritic growth would occur thus enabling the position and shape of the interface to be determined. As will be shown later breakdown did not in fact occur.

There are five sets of compositional readings present on figure 8. The solid triangles are calculated from the densities of 2 mm wide wafers cut from the boule. These represent an average composition over that entire volume. Due to the need to cut in other orientations, density reading were made only near the beginning and end of the boule. The ampoule is conical so that the first to freeze material is of smaller diameter; density reading were not made. The other four sets of readings were taken with energy dispersive analysis, utilizing the HgM, CdL and TeL x-ray emission lines. The scanning electron microscope was used in the spot mode with 10 keV accelerating potential. Despite the fact that the surfaces were curved good totals were obtained between 99 and 101% after ZAF (atomic number, absorption, fluorescence) corrections were made. The J7 position referred to in figure 8 indicates an electrical jack on the furnace which pointed directly toward the front of the orbiter. This location was carefully tracked during the opening of the cartridge and the subsequent dissolution of the fused silica ampoule in hydrofluoric acid. Of specific interest is that each surface exhibits a different compositional trend, particularly over the first half of the growth. The J7 + 90 position consistently has a high x value, while the J7 and J7-90 positions are consistently lower. It should also be noted in this region that the density readings are lower than any of the surfaces and that they do follow the calculated diffusion data. In this sense they are similar to the ground testing.

At the position corresponding to the rate change, there is an obvious drop in the x-value corresponding to the inability of the boundary layer to be replenished by cadmium fast enough to maintain equilibrium solidification. Figure 8 is an etched region through this part of the material, and there is no indication of dendritic growth or breakdown; in fact the grains continue to grow through both the rate changes. Following the initial drop in composition, there is an increase in the cadmium content when the material reverts to the original slower rate. Following the second attitude change at MET 8/00:30 it can be seen that all the surface curves deviate not only from the position of the diffusion controlled tendency, but also from the shape. Furthermore, the EDS readings indicate that the surface CdTe concentration is lower than the mean value indicated by density. This is the opposite of the normal tendency, and is indicative of complete mixing. Cross sections of material from this area have not been made yet, but the indication is that there is more radial homogeneity than would normally be seen in this material during the final transient.

Figure 7 shows the OARE data transcribed to the cross sections of the crystals during the 3 main attitude periods of the mission. The data are shown in the form of the resolved component parallel to the interface, and also the vector perpendicular to the interface. As can be seen in the first and third attitudes, this latter was unfavorable. The results exhibit considerable radial asymmetry in the first attitude; the degree of inhomogeneity is in fact worse

than in the ground based equivalent experiment. Figure 9 shows a cross section of the crystal grown in the first and second attitudes. The first attitude (+YVV/-ZLV) gives rise to very inhomogeneous material despite the low total vector. This sample is, in fact, worse than normally seen on the ground and worse than the ground truth sample run to simulate the mission. Clearly the second attitude with the vector in a favorable direction is more homogeneous. In both attitudes one can see a tendency for the heavier HgTe-rich material to be aligned with the vector. This a clear indication of three dimensional fluid flow. In this case of the material grown in the -XLV/-ZLV attitude the material is much more homogeneous. Even though the transverse vector is three times as large (1.55 μg_0 versus 0.55 μg_0), the perpendicular vector is stabilizing and so the material is more uniform. The ratio of perpendicular to transverse is very low, on the order of 0.3. Ideally this ratio would be at least 4:1. The material is still nothing like as uniform as would be achieved with diffusion control, and, for the same temperature profile, is inferior to that produced by growth in an axial magnetic field.[10] Nevertheless, the improvement is clearly the result of a reduction of the fluid flow. With improved microgravity conditions, including a much reduced transverse vector and a perpendicular to transverse ratio of 4:1, conditions closer to diffusion control can be obtained. This is one of the objectives of further microgravity missions. The first mission has clearly shown the effect of three dimensional fluid flow on the solidification characteristics of a material such as this having a wide separation between the liquidus and the solidus.

6. ACKNOWLEDGMENTS

The authors are indebted to C. Bahr, D. Lovell, J. M. Jones and G. Nelson for their dedicated technical assistance, particularly in the fields of furnace fabrication and operation and glass-blowing. The design and fabrication of the AADSF by personnel at MSFC and Teledyne Brown Engineering has made this project possible. The support, both moral and financial of the Microgravity Science and Applications Division at NASA Headquarters has been enthusiastic, warm and helpful.

7. REFERENCES

1. F. R. Szofran and S. L. Lehoczky, "The Pseudobinary HgTe-CdTe Phase Diagram," *J. Electronic Malts., 10, 1131-1150*, 1981.

2. D. H. Kim and R. A. Brown, "Models for Convection and Segregation in the growth of HgCdTe by the vertical Bridgman method," *J. Crest. Growth, 96, 609-627*, 1989.

3. A. V. Bune, D. C. Gillies, D. A. Watring and S. L. Lehoczky, "Modeling of Convection and Segregation during HgCdTe Directional Solidification with Emphasis on Coupling with Crystal-Melt Interface," to be presented at *Tenth American Conference on Crystal Growth*, Vail, CO August 4-9, 1996.

4. K. Mazuruk, Ch.-H. Su, S. L. Lehoczky and F. Rosenberger, " Novel oscillating cup viscometer - application to molten HgTe and $Hg_{0.8}Cd_{0.2}Te$," *J. Appl. Phys. 77 (10)*, 15 May 1995.

5. L. R. Holland and R. E. Taylor, "Measured Thermal Diffusivity of $Hg_{1-x}Cd_xTe$ Solids and Melts," *J. Vac. Sci. Technol., A1 (3), 1615-9*, 1983.

6. D. Chandra and L. R. Holland, "Density of liquid $Hg_{1-x}Cd_xTe$," *J. Vac. Sci. Technol.*, A1(3), 1620-4, 1983.

7. J. C. Clayton, M. C. Davidson, D. C. Gillies and S. L. Lehoczky, "One Dimensional Analysis of Segregation in Directionally Solidified HgCdTe," *J. Cryst. Growth, 60, 374-80*, 1982.

8. D. C. Gillies, F. A. Reeves, L. B. Jeter, J. D. Sledd, J. M. Cole and S. L. Lehoczky, "The advanced Automated Directional Solidification Furnace," *SPIE, This meeting*, 1996.

9. J. E. LeCroy and D. P. Popok, "Design of a High Thermal Gradient Furnace," *32nd Aerospace Sciences Meeting and Exhibit, AIAA 94-0336*, Reno NV, 1994.

10. D. A. Watring, S. L. Lehoczky, F. R. Szofran and D. C. Gillies, "Convective Influence on Radial Segregation During Unidirectional Solidification of the Binary Alloy, HgCdTe," *SPIE, This meeting*, 1996.

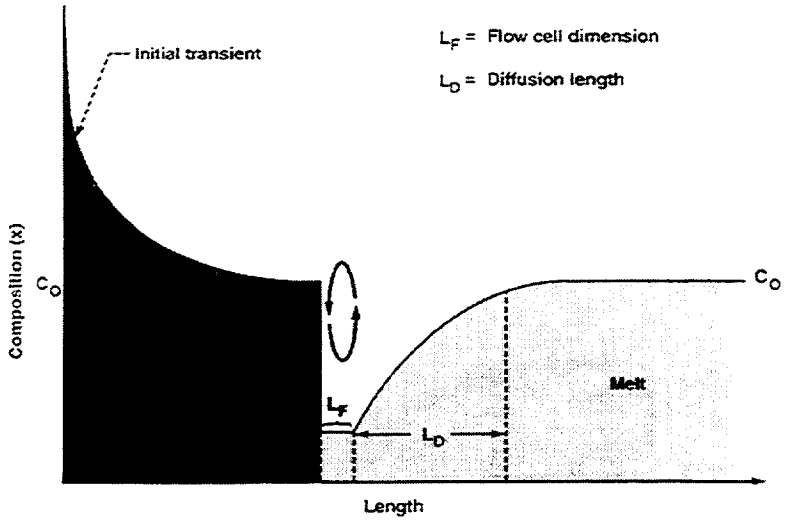

Figure 1. Interface Region showing Convective Cells

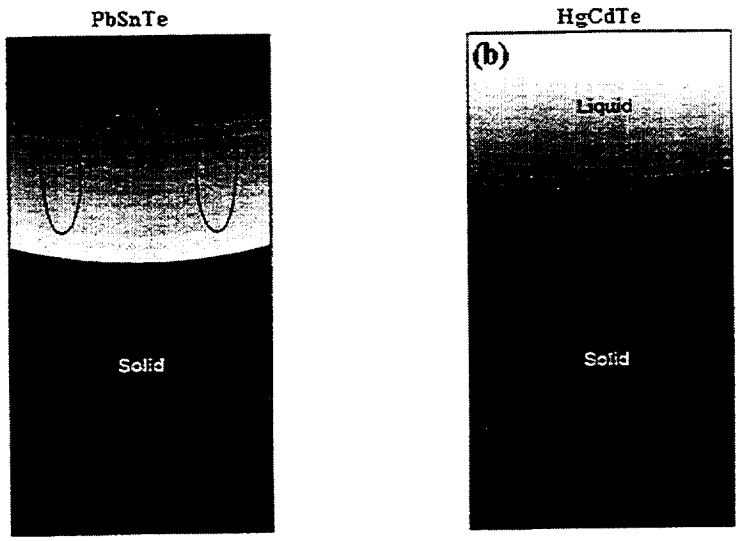

Figure 2. Gravity Effects in the Solidification of Pseudobinary Solid Solution Systems. (a) Rejected component less dense than bulk liquid results in thermosolutal convection throughout the liquid volume. (b) Rejected component more dense than bulk liquid results in interface shape instability in presence of radial temperature gradient.

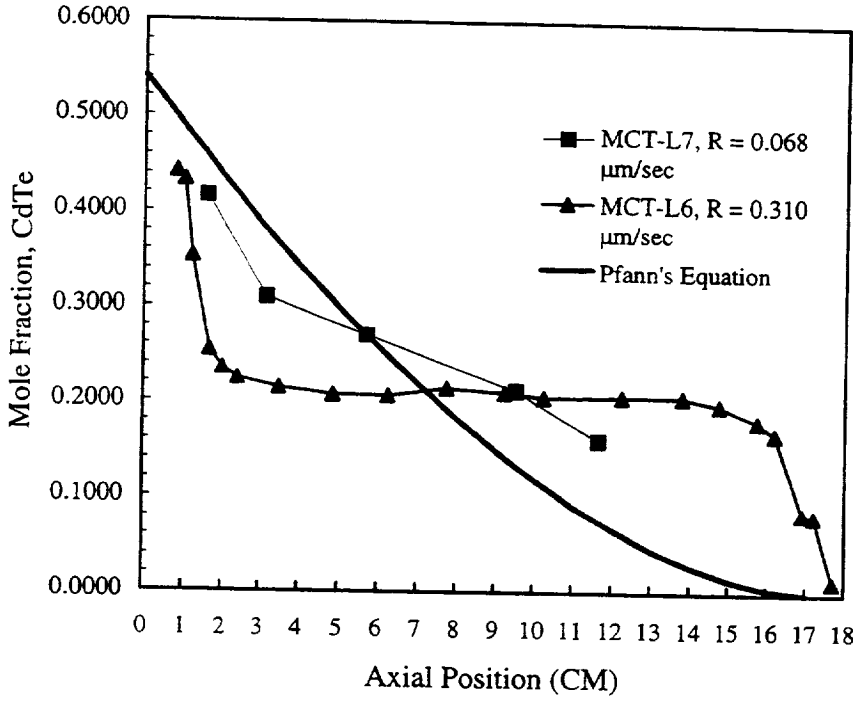

Figure 3. CdTe Compositional Distribution for Two Different Growth Rates

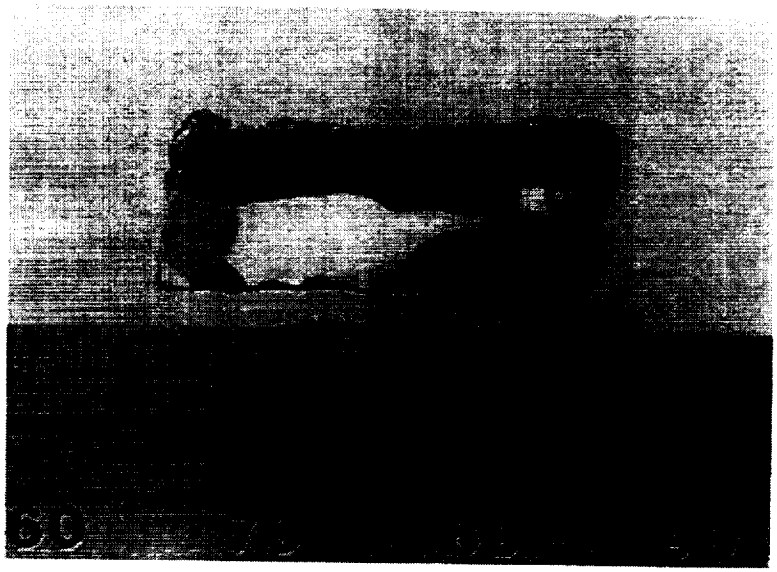

Figure 4. Typical Quenched-in Interface in HgCdTe

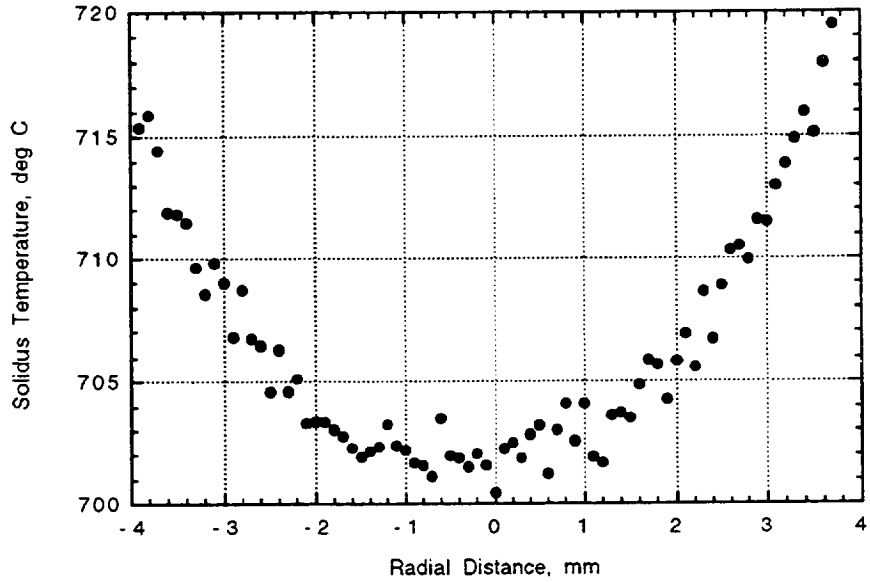

Figure 5. Temperature of Solidification at Interface

Orbiter Attitude	Transverse Residual Acceleration	Residual Axial Acceleration	Resolved Transverse	Axial/Transverse Ratio	Total Resolved
-ZLV/+YVV 0 - 9 cm	J7 0.53 0.15	Hot 0.28 Cold	16° 0.55	-0.51	0.62
-XLV/-ZVV 9 - 11 cm	J7 0.28 1.53	Hot 0.50 Cold	1.55 10°	+0.32	1.63
-XLV/+ZVV 11 - 15 cm	J7 0.28 1.42	Hot 0.43 Cold	1.45 11°	-0.31	1.51

Figure 6. Orbiter attitudes and residual acceleration vectors AADSF during USMP-2

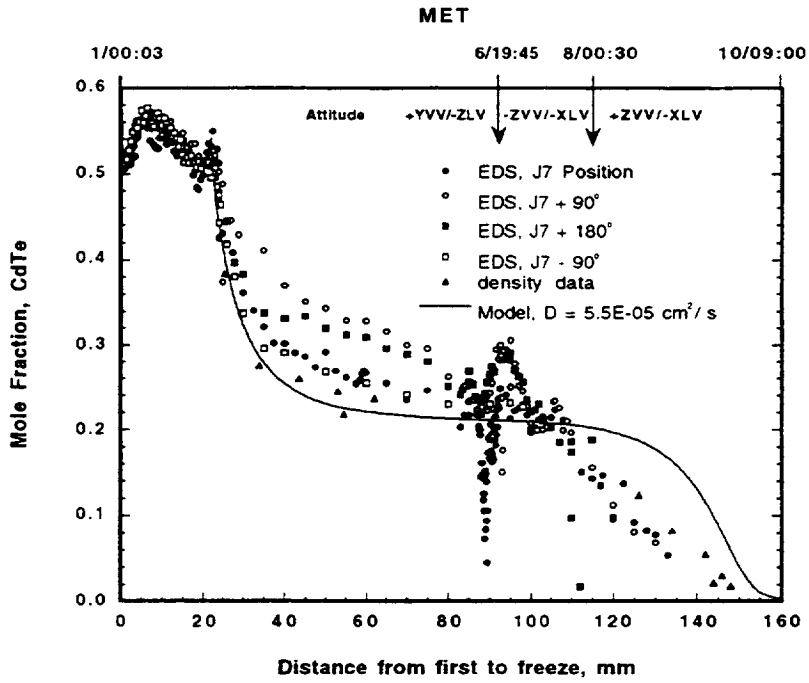

Figure 7. Mission Timeline for USMP-2 Showing Composition of Crystal Grown

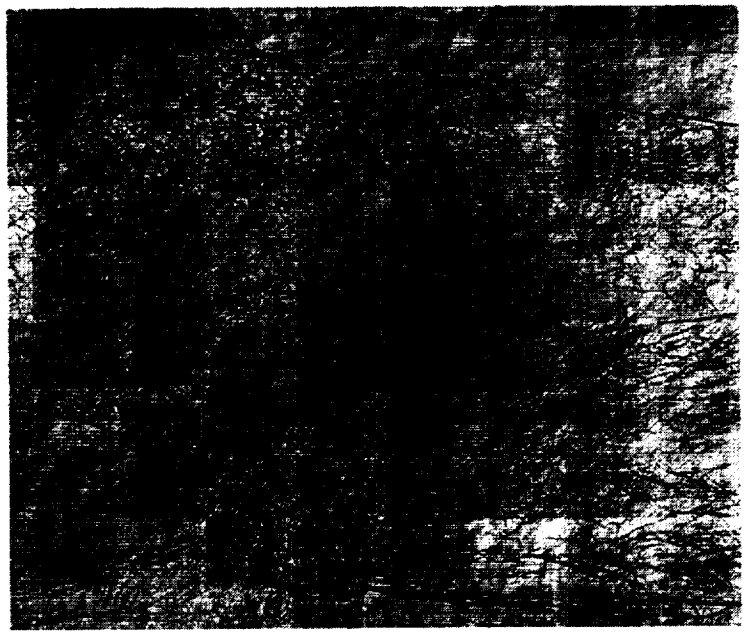

Figure 8. Microstructure of HgCdTe during the Rate Change (etched in Polisar II)

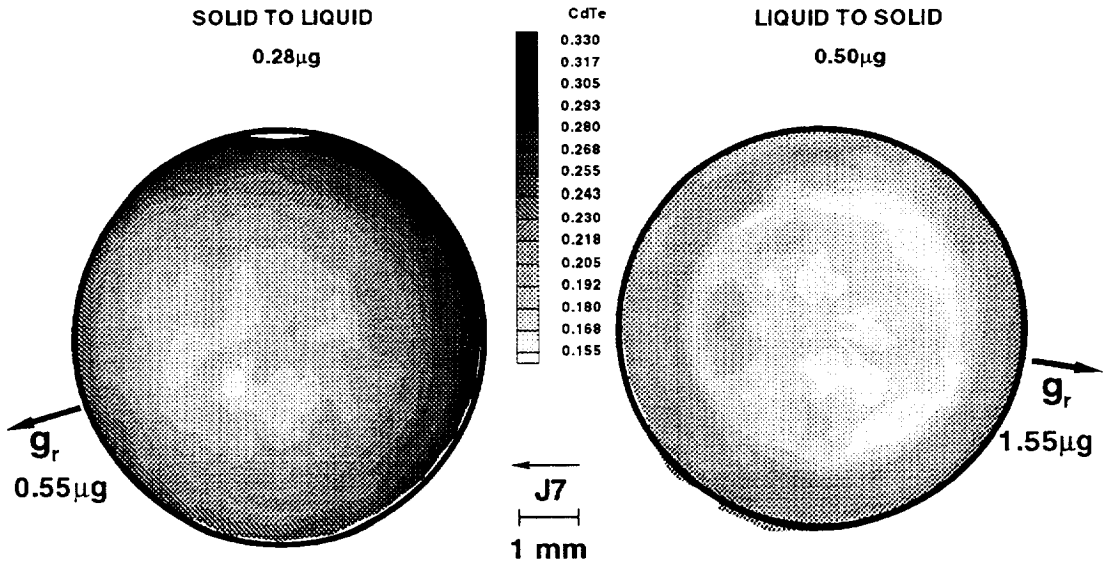

Figure 9. Compositions of Material Grown During two Attitudes of the Orbiter